Reactive growth of MgO overlayers on Fe(0 0 1) surfaces studied by low-energy electron diffraction and atomic force microscopy

Antoni Tekiel [a,*], Shawn Fostner [a,b], Jessica Topple [a], Yoichi Miyahara [a], Peter Grütter [a]

[a] Physics Department, McGill University, 3600 University Street, Montreal, QC, H3A 2T8 Canada
[b] Department of Physics and Astronomy, University of Canterbury, Private Bag 4800, Christchurch 8140, New Zealand

ABSTRACT

Ultra-thin MgO films grown reactively on the Fe(0 0 1) surface by evaporation of magnesium in an atmosphere of molecular oxygen have been investigated by low energy electron diffraction and non-contact atomic force microscopy. Preparation of structurally stable crystalline films requires a protocol that prevents an excessive interfacial reaction between oxygen and the Fe(0 0 1) surface, but at the same time provides a sufficient amount of oxygen in order to grow a stoichiometric MgO film. The proper ratio between the magnesium deposition rate and the oxygen pressure has been determined, as well as measures to prevent initial interfacial oxidation of the substrate. The effect of both post-annealing and an increased substrate temperature during the growth has been studied. We demonstrate that the reactive deposition method, which gives full control over the gaseous species that reach the surface, can produce terraces that have an average size of 10 nm (on an 8 monolayer thick film), which is a significant improvement compared to other preparation methods, such as thermal or electron beam evaporation of MgO.

© 2013 Elsevier B.V. All rights reserved.

1. Introduction

Magnesium oxide ultra-thin films grown on a variety of metal substrates, such as Ag(0 0 1), Mo(0 0 1) and Fe(0 0 1), play important roles in magnetoelectronics [1] and in systems for studying model catalysis [2]. Ultra-thin MgO films that serve as a tunneling barrier have been identified as a promising building block of magnetic tunnel junctions (MTJs). In the case of Fe(0 0 1)/MgO/Fe(0 0 1) MTJs, crystalline MgO leads to a high tunneling magnetoresistance ratio (TMR) [3,4]. The quality of the MgO interface is pivotal to TMR, and thus for more than a decade there has been growing interest in improving the quality of MgO films on the Fe(0 0 1) surface, in order to further increase the TMR to much higher values predicted theoretically [5,6]. However, even the best films are still characterized by a high number of defects, such as dense networks of misfit dislocations and very small terraces (understood as flat areas separated by atomic steps). The terraces of MgO films deposited at room temperature are only a few nanometers in width [7,8] and are smaller than the separation between dislocations. High-resolution characterization by scanning probe microscopy of MgO films on Fe(0 0 1) prepared at elevated temperatures is very limited [8] and consequently, it is still an open question how such a preparation method

can improve their quality. Evaporation at higher sample temperatures and post-annealing have been beneficial for the quality of MgO films on Ag(0 0 1) [10] leading to larger terraces. Also in the case of MgO films on Mo(0 0 1) [11] annealing reduces the density of step-like features formed due to dislocations.

The reduction in quality of MgO films on Fe(0 0 1) surfaces can be attributed to the conventionally used preparation method and the fact that iron is very prone to oxidation. In an ultra-high vacuum (UHV) environment, MgO films are usually deposited onto the Fe(0 0 1) surface by electron beam evaporation of a stoichiometric MgO target [4,7] and the resulting beam is composed mainly of magnesium and oxygen, both in an atomic form [9]. However, on Ag(0 0 1) and Mo(0 0 1) surfaces MgO thin films with the best morphology have been obtained by the reactive deposition of Mg in an O_2 atmosphere, the rate and pressure of which can be independently controlled [10,11], in contrast to the electron beam evaporation. Both methods are quite challenging experimentally, as MgO is essentially grown from two separate sources of magnesium and oxygen, which must react on the substrate in order to nucleate MgO molecules (in case of molecular oxygen, an O_2 molecule has first to dissociate). Next, MgO molecules diffuse and build MgO islands. There are three stages of such growth, each potentially requiring different growth parameters, as it is taking place on a dissimilar substrate: (i) growth of the 1st monolayer, (ii) growth of several consecutive layers under conditions perturbed by the metallic substrate and (iii) growth of bulk-like MgO. The

* Corresponding author. Tel.: +1 5143986749.
  E-mail address: antoni.tekiel@mail.mcgill.ca (A. Tekiel).

reactive deposition method provides direct control of the relative exposure of the sample to magnesium and oxygen. For instance, this is exploited on the Ag(0 0 1) surface, where an overexposure of the surface to oxygen can be used to prevent an unwanted reaction between silver and magnesium [12]. Similarly, during the reactive growth of MgO on the Fe(0 0 1) surface, the amount of oxygen to which the iron surface is exposed can be precisely controlled. Although the formation of an FeO_x interface may reduce the TMR in MTJs [13,14], the oxygen at the Fe/MgO interface can facilitate epitaxy of MgO thin films on Fe(0 0 1) [15]. The exposure to a very small amount of molecular oxygen (below 1 ML) does not change the substrate morphology drastically, as it leads to an immediate dissociation of oxygen molecules that preferentially absorb in four-fold hollow sites of the Fe(0 0 1) surface [16]. Based on scanning tunneling microscopy characterization, Bonell et al. [17] suggested that at this coverage range the oxygen remains mobile on the surface. When approaching a full monolayer, oxygen atoms reveal high degree of ordering leading eventually to a $p(1 \times 1)$-O reconstruction with each hollow site of the Fe(0 0 1) surface occupied by one oxygen atom. However, if this exposure amount is exceeded, poorly defined iron oxide islands of 2–3 ML thickness are formed [18], which will significantly disturb subsequent MgO growth. This means that during reactive growth there should exist a particular composition of the flux reaching the sample that can form a well-ordered MgO monolayer, even if the iron substrate has been in contact with oxygen and might have been partially oxidized. During the growth of the consecutive MgO layers, the amount of oxygen should be increased, as the iron substrate has been already covered and a higher oxygen concentration is required to grow a stoichiometric MgO film.

So far, the reactive growth of MgO on Fe(0 0 1) has been studied only by high resolution electron energy loss spectroscopy [19], photoelectron spectroscopy [20,21], and at 1 ML coverage by scanning tunneling microscopy [22]. In this study we focus on the reactive growth method of 8–16 ML thick MgO films, which are characterized here both in real and reciprocal space. This thickness range is typically used in magnetic tunnel junctions [1] and in systems for studying model catalysis, where the MgO film supports metal nanoparticles [2]. In order for such a film to have high crystalline quality, the film must be successfully grown at all three steps mentioned above. The composition of the flux can be easily varied at the timescale needed to grow one MgO monolayer by controlling the gaseous species deposited, allowing for readjustment of parameters at each step of the growth process. We use low energy electron diffraction (LEED) to determine the quality of MgO films grown from fluxes of different compositions and at various sample temperatures. Excessive oxidation of the Fe(0 0 1) substrate can be avoided by decreasing the oxygen pressure at the beginning of the growth or by the deposition of a submonolayer Mg prior to the reactive growth of MgO. Characterization by non-contact atomic force microscopy (NC-AFM) of an 8 ML thick film demonstrates that compared to deposition by electron beam evaporation of MgO, the reactive growth can produce a better ordered surface with larger terraces.

2. Methods

All experiments reported here are performed in two interconnected UHV chambers (preparation and microscope) based on a commercial JEOL JSPM 4500a UHV AFM system. The base pressure is in the low 10^{-11} mbar range in the preparation, and 1×10^{-10} mbar in the microscope chamber. Iron whiskers home-grown by reduction of $FeCl_2$ in an H_2 atmosphere with {0 0 1} side-surface orientations are used as the starting substrate [23]. The whiskers are cleaned by several cycles of 1 keV Ar^+ sputtering and

a subsequent annealing to about 600 °C until a clean LEED pattern is observed. This procedure leads to a surface with terraces several hundred nanometers wide. A piece of magnesium (99.99% purity) is outgassed in vacuum and then evaporated from a Knudsen cell onto the Fe(0 0 1) sample kept at temperatures ranging from room temperature (RT) to 300 °C in an atmosphere of molecular oxygen (99.997% purity), whose pressure is controlled by a high precision leak valve. The rate of magnesium deposition was monitored by quartz crystal microbalance and the MgO coverage was deduced from a rescaled value due to the density difference between the films of Mg and MgO. Long-range order of the evaporated layers is characterized by LEED performed at room temperature. Although electrons can cause desorption of oxygen from the MgO(0 0 1) surface, this effect is very small at low electron energies and has a threshold at 55 eV incident electron energy [24]. Also no time deterioration of LEED images recorded at 90–150 eV electron energy has been observed in this work. Non-contact atomic force microscopy is also carried out at room temperature in the frequency modulation (FM) mode using JEOL AFM and Nanosurf 'easyPLL' frequency detector/oscillation controller in self-oscillation mode. Commercial Nanosensors PPP-NCLR silicon cantilevers with a typical resonance frequency of 150–160 kHz and spring constant of $\approx$42 N m^{-1} are used with a peak-to-peak oscillation amplitude of 10–14 nm. A constant bias voltage during NC-AFM imaging was applied to the sample to compensate long-range electrostatic forces.

3. Results and discussion

After the sputter-cleaning procedure the Fe(0 0 1) surface was examined by LEED and NC-AFM (see Fig. 1(a)). The LEED pattern reveals very clear (1×1) symmetry. The surface is composed of atomically flat terraces of typical size exceeding 100 nm, and locally up to 500 nm. If the clean Fe surface is exposed to 6 L (Langmuir, $1 L = 10^{-6}$ Torr s) of O_2 at RT, there is almost no change in the quality of the LEED pattern, and similarly the presence of oxygen is not directly evidenced by AFM, which is related to mobile oxygen on the surface. With an 8 L dose, the LEED pattern vanishes almost completely and the surface roughness increases due to formation of iron oxide islands. Such a morphology, which has been characterized by Parihar et al. using surface X-ray diffraction [18], is undesirable for subsequent growth of MgO. The fact that this unwanted morphology forms first at the dose of approximately 8 L can be used to estimate a lower limit for the deposition rate of Mg. For instance, at a pressure of 1.33×10^{-7} mbar (1×10^{-7} Torr), a dose of 8 L corresponds to an exposure duration of 60 s (at this pressure 1 ML of O_2 should form after about 4 s assuming sticking coefficient of 1 [25]). If during that time a sufficient amount of Mg atoms arrive at the surface to form the first MgO monolayer, the unwanted morphology shown in Fig. 1(b) should not form. In other words, the time needed to form the first MgO monolayer should be shorter than the exposure time that is equivalent to 6–8 L at a given O_2 pressure. Usually magnesium is deposited at a rate of approximately 1 Å/min (0.38 ML/min) during the reactive growth on Ag(0 0 1) and Mo(0 0 1) surfaces. Assuming that $n_{Mg}/n_{MgO} \approx 1$, where n_{Mg} and n_{MgO} denote the number of Mg atoms per unit area in *hcp* Mg(0 0 0 1) and *rock-salt* MgO(0 0 1) monolayers, respectively, formation of an MgO monolayer requires approximately 160 s, at shortest. This gives a rough estimation of 5×10^{-8} mbar for the maximum oxygen background pressure during the reactive growth at a Mg deposition rate of 1 Å/min.

We next utilize LEED to investigate the effect of the Mg deposition rate and the background pressure of the oxygen atmosphere on the crystalline quality of MgO thin films on Fe(0 0 1). Fig. 2 shows LEED patterns of 8 ML thick MgO samples grown at RT and prepared at O_2 pressures ranging from 1×10^{-8} to
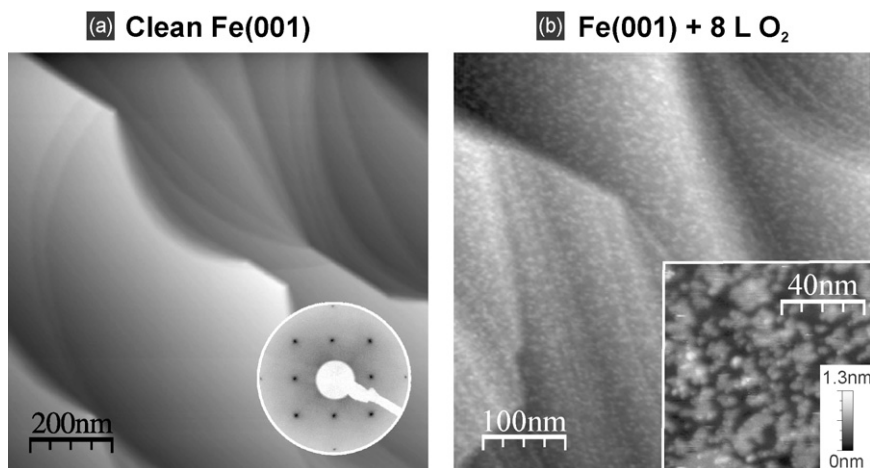
(a) Clean Fe(001)   (b) Fe(001) + 8 L O₂

Fig. 1. (a) A clean Fe(0 0 1) whisker surface: NC-AFM topographical image recorded at $\Delta f = -18$ Hz and sample bias 0 V, LEED pattern recorded at 141 eV electron energy. (b) The Fe(0 0 1) surface after the exposure to 8 L of O₂ showing formation of iron oxide islands (parameters of both frames: $\Delta f = -3$ Hz, sample bias 0.5 V).

6×10^{-7} mbar, and Mg deposition rates 1.0–3.6 Å/min, as suggested by the previous estimation. A series of samples grown at Mg deposition rates 1.3–1.5 Å/min indicates that the LEED patterns become sharper if the O₂ pressure is within a range of 5×10^{-8} and 5×10^{-7} mbar, confirming a well-ordered crystal structure and an epitaxial growth of the MgO film. Both for lower (1×10^{-8} mbar) and higher (5×10^{-7} mbar) O₂ pressures the LEED patterns start to fade away. For higher Mg deposition rates, this interval of optimal growth parameters is shifted towards higher O₂ pressures, and for lower Mg deposition rates, to lower O₂ pressures. Based on those observations, two regions of unfavorable growth parameters can be identified. The first region is related to the oxidation of the Fe(0 0 1) surface and occurs for higher pressures of O₂. The second region is characterized by a high rate of Mg deposition and an amount of oxygen that is insufficient to grow a stoichiometric MgO film. Thus, the crystal structure is optimized for a particular ratio $r/p = 0.15 \pm 0.05$

between the Mg deposition rate (r, expressed in Å/min) and the O₂ pressure (p, expressed in 10^{-8} mbar).

Although well-ordered films can be prepared by using constant Mg deposition rates and O₂ pressures, not all of such MgO films retain high quality after annealing. Such structural instability is most likely related to the balance between the oxidation of the substrate at the MgO/Fe interface and MgO film stoichiometry. This suggests that constant r and p parameters cannot fulfill simultaneously optimal conditions for avoiding the overoxidation of the Fe substrate surface and maintaining the stoichiometry of MgO thereafter. Higher substrate temperatures applied during or after the growth usually lead to larger terraces, which is highly desirable in case of the MgO/Fe system. In order to circumvent this limitation, two solutions were tested, both providing similar positive results: (i) reducing the O₂ pressure at the beginning of the growth for a duration needed to grow the 1st MgO ML; and (ii) deposition of a submonolayer of Mg prior to the reactive growth of MgO. Alternatively, the r/p could be controlled by varying the angle at which Mg is evaporated, and effectively changing its deposition rate. Fig. 3(a) shows a 16 ML thick MgO film that was deposited at RT onto 0.3 ML of Mg with the oxygen pressure during the formation of the first MgO ML 1.3×10^{-7} mbar, and increased to 5×10^{-7} mbar thereafter (at the Mg deposition rate of 2.2 Å/min). Directly after growth, the sample is characterized by
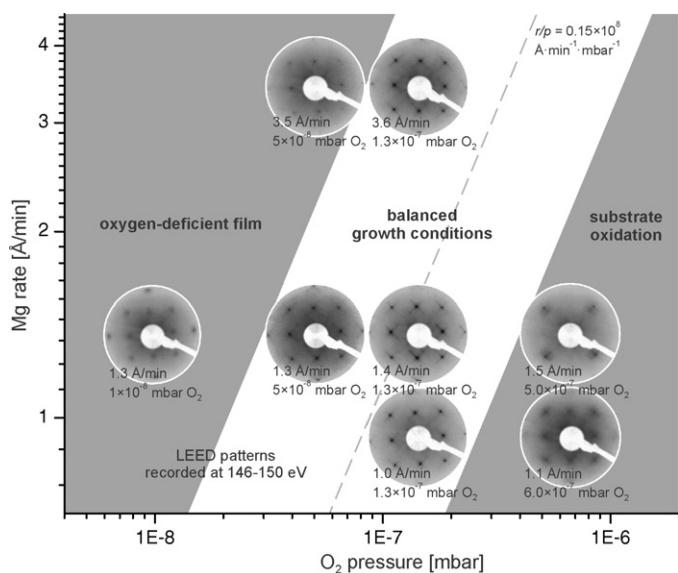

Fig. 2. LEED patterns of 8 ML thick MgO samples grown at RT and prepared at various O₂ pressures and Mg deposition rates. MgO films reveal higher crystalline order for a particular ratio $r/p = (0.15 \pm 0.05) \times 10^8$ Å min⁻¹ mbar⁻¹ between the Mg deposition rate and the O₂ pressure. There are two regions of unfavorable growth parameters. The first region is related to the oxidation of the Fe(0 0 1) surface and occurs for higher pressures of O₂. The second region is characterized by a high rate of Mg deposition and an amount of oxygen that is insufficient to grow a stoichiometric MgO film.
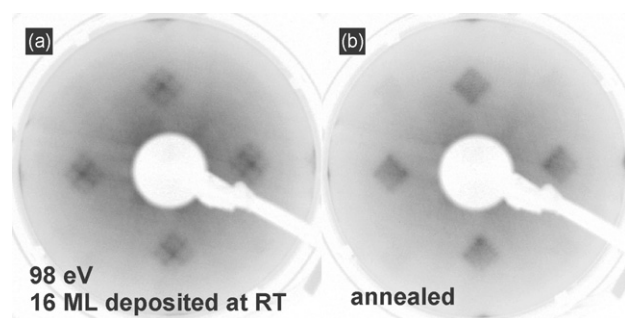

Fig. 3. 16 ML thick MgO film deposited at RT onto 0.3 ML of Mg with the oxygen pressure during the formation of the first MgO ML 1.3×10^{-7} mbar, and increased to 5×10^{-7} mbar thereafter (at the Mg deposition rate of 2.2 Å/min). (a) LEED pattern of an as-deposited sample shows additional satellite spots around main MgO diffraction spots revealing 4 equivalent angles, characterizing the warped MgO surface above misfit dislocation lines. (b) LEED pattern after annealing at 400 °C for 20 min showing instead a subatomic modulation of the height of the MgO film. The change in surface topography is further analyzed during the discussion of Fig. 6, which features a real space image of the MgO film after annealing.
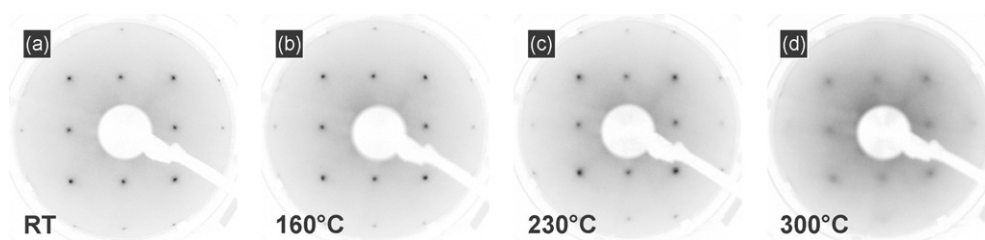
Fig. 4. LEED patterns of 8 ML thick MgO films grown at temperatures from RT to 300 °C (recorded at 141–145 eV electron energy). The O_2 pressure was 1.3×10^{-7} mbar during the formation of the 1st MgO ML, and increased to 5×10^{-7} mbar thereafter (at the Mg deposition rate of 2.0–2.5 Å/min). A higher crystalline order characterizes samples grown from RT up to 160 °C. At 230 °C the order is slightly reduced, with a significant decrease at 300 °C.

high crystalline order with misfit dislocations [26–28] revealed by additional satellite spots around the main MgO diffraction spots. After annealing at 400 °C for 20 min, the background in the LEED pattern is reduced, and there is a change in the appearance of the diffraction spots splitting (see Fig. 3(b)). On as-deposited samples, there are four equivalent angles characterizing the warped MgO surface above misfit dislocation lines, giving rise to distinct satellite spots connected with the main MgO spots by weak lines. After the annealing there is instead a broad distribution of angles revealing a subatomic modulation of the height of the MgO film, which may originate from rearrangement at the MgO/Fe interface leading to local deformation of the crystalline lattice. The change in surface topography is further analyzed during the discussion of Fig. 6, which features a real space image of the MgO film after annealing.

The temperature of the sample during the reactive growth is one of the important parameters determining the resulting film morphology. Usually an increased temperature helps in overcoming energy barriers for diffusion of adsorbates and leads to

formation of larger islands. Fig. 4 shows 8 ML thick MgO films grown at four different sample temperatures ranging from RT to 300 °C (at the Mg deposition rate of 2.0–2.5 Å/min). A higher crystalline order characterizes samples from RT to 160 °C. At 230 °C the order is slightly reduced, with a significant decrease at 300 °C. Such a change can be caused by the interfacial oxidation of the iron substrate, which is enhanced at higher temperatures, showing that the prevention measures based on changing the r/p ratio require even further modification during the initial stage of the growth. At elevated temperatures, other effects may also play an important role, such as (inter) diffusion of substrate and film atoms at the MgO/Fe interface and re-evaporation/desorption of Mg.

A large-scale NC-AFM image of an 8 ML thick MgO film deposited at 90 °C is shown in Fig. 5(a). The surface is almost uniformly covered with the MgO film. An enlarged frame of the same film presented in Fig. 5(b) shows an interface characterized by multiple dislocation lines and atomic step edges, running preferentially parallel to the $\langle 110 \rangle$ directions of the iron substrate. In Fig. 5(c)
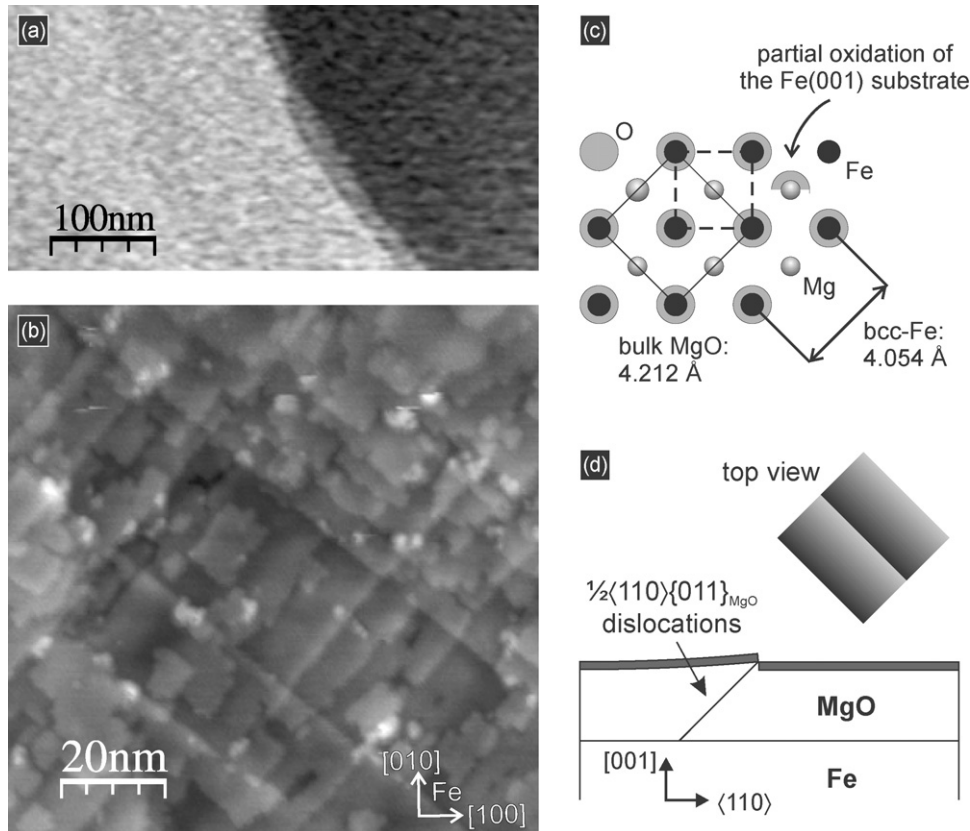

Fig. 5. (a) A large-scale NC-AFM image of an 8 ML thick MgO film ($\Delta f = -2$ Hz, sample bias 2 V). (b) An enlarged NC-AFM frame showing an interface with directional step edges that are predominantly formed due to misfit dislocations ($\Delta f = -5$ Hz, sample bias 2 V). (c) A schematic diagram of the MgO/Fe registry. (d) The glide of $\frac{1}{2}\langle 011 \rangle$ dislocations on $\{011\}_{MgO}$ planes of the MgO film produces a monoatomic step at the surface.
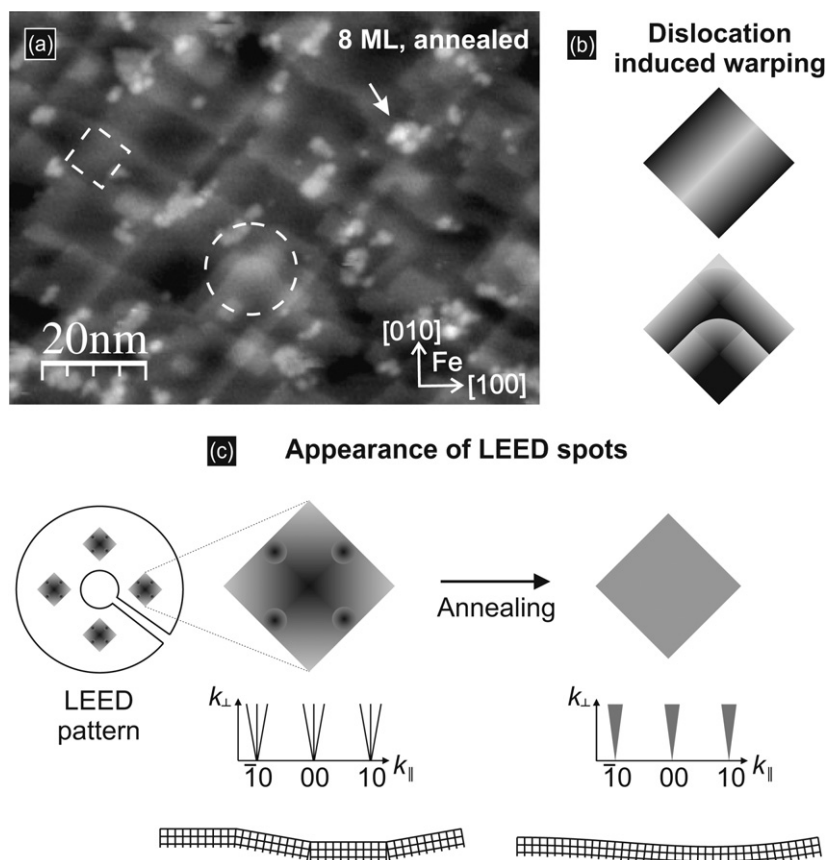
Fig. 6. (a) NC-AFM image of an 8 ML thick MgO film after annealing at 400 °C. The arrow indicates unidentified features, which can be attributed to an excess magnesium that segregated on the surface after the annealing ($\Delta f = -2$ Hz, sample bias -2 V). (b) Additional warping of the surface formed after the annealing (exemplified by areas marked by the square and the circle in panel (a)). (c) Change in the appearance of LEED spots before and after the annealing (compare with Fig. 3). After the annealing the well-defined satellite peaks in LEED spots in Fig. 3 almost disappear leading only to a square-like shape that has a smaller size, which indicates a reduced maximum angle characterizing the distortion of the MgO film.

a schematic diagram of the MgO—Fe registry shows that such an orientation corresponds to a charge neutral —Mg—O—Mg— termination, which confirms the orientation of the MgO film independently from the LEED measurements. Although the film appears to be rough, not all step edges lead to a real increase of the MgO film height and can instead be attributed to misfit dislocations. As revealed by the additional satellite spots in the LEED images (Figs. 2 and 3), the MgO film contains a dense network of misfit dislocations that induce a warped MgO surface above them. This mechanism of strain relief has been discussed in detail by Dynna et al. [26] and is schematically presented in Fig. 5(d). Using MgO as a reference system, the glide of $\frac{1}{2} \langle 0\,1\,1 \rangle$ dislocations on $\{0\,1\,1\}_{MgO}$ planes of the MgO film produces a monoatomic step at the surface. The average dislocation periodicity is about 10 nm, which is close to the expected value of ~11 nm ($a_{MgO} \cdot a_{Fe}/|a_{MgO} - a_{Fe}|$, where $a_{MgO} = 4.212$ Å, and $a_{Fe} = 4.054$ Å – see Fig. 5(c)). The surface is also characterized by atomic terraces of a similar size. Locally, the distance between dislocation lines can be as large as 20 nm allowing for the formation of larger terraces.

The effect of post-annealing on the morphology of MgO films has been already demonstrated in Fig. 3 using LEED measurements, which indicated an induced subatomic modulation of the MgO film height after annealing. To complement this, Fig. 6(a) shows an NC-AFM image of an 8 ML thick MgO film annealed at 400 °C. Compared to Fig. 5(b), annealing leads to an increase in the average distance between dislocation lines. Also, the MgO surface seems to be better ordered, as the number of atomic MgO islands is slightly reduced, and frequently the size of flat MgO areas is limited by the

separation of dislocation lines. The subatomic modulation of the film height can be directly observed in Fig. 6(a) in the area indicated by a square. Such warping of the surface most likely happens due to overgrowing of the dislocation planes, which were schematically shown in Fig. 5(d), however the buried interface itself cannot be probed directly by NC-AFM. Before the annealing, the surface of the MgO film is usually bent around four equivalent $\langle 0\,1\,1 \rangle$ directions as shown in Fig. 5(b), which leads to a characteristic cross-like shape of the LEED spots (see Figs. 3 and 6(c)). In contrast, after the annealing the MgO surface is twisted also around other directions (see Fig. 6(a)), which is caused by overgrowing of the dislocation planes and formation of surface features shown in Fig. 6(b). This additional distortion leads effectively to a less directional warping of the film height and consequently, the well-defined satellite peaks in the LEED image in Fig. 3 almost disappear leading only to a square-like shape (see Fig. 6(c)). The distinct shape of LEED spots indicates that there is a well-defined maximum angle characterizing the distortion of the MgO film. In particular, the square-like shape reveals that there is an anisotropy in the warping of the surface, which is related to the fourfold symmetry of the surface. After the annealing the square-like LEED spots become smaller, which confirms flattening of the film (see Fig. 6(c)). One should also note that on samples fabricated under conditions leading to a slightly oxygen deficient film (see Fig. 2, occasionally the quality of an initially sharp LEED pattern can deteriorate significantly after annealing. In this case annealing can force the excess magnesium to diffuse and segregate on the surface in the form of clusters. Such metallic clusters, which can be electrically charged and repel the incoming beam of electrons,

disturb significantly LEED measurements. In such a situation, the film can be well-ordered, but the LEED pattern will be very fuzzy. Although the sample in Fig. 6(a) was grown under optimal conditions, there are some unidentified features (marked by an arrow), which can be attributed to an excess magnesium that segregated on the surface after the annealing. However, due to a small amount of such clusters, they did not hinder the LEED measurements.

The presented protocol to grow epitaxial MgO films on the Fe(0 0 1) surface by reactive deposition can produce an interface with well-ordered terraces and a much higher quality compared to the growth by electron beam evaporation. In this way, by taking a special precaution to avoid the interfacial reaction between the iron surface and the oxygen background atmosphere, films resembling the quality of MgO overlayers on Mo(0 0 1) and Ag(0 0 1) surfaces are formed [10,11]. The reactive deposition method allows for full control over the gaseous species that reach the surface, making this protocol easily reproducible in various experimental settings. Conversely, the electron beam evaporation can be realized in two configurations, where the evaporated target is either grounded or biased at a high positive voltage [7,29]. Because such a beam is composed of two species [9], not necessarily in the same charge state, the exact design of the evaporator (which can be equipped e.g. with retarding grids) can decide the resulting beam composition. An interesting example is the growth of MgO by electron beam evaporation on Ge(0 0 1) studied independently by Han et al. [30] and Jeon et al. [31]. Although both groups used almost the same MgO deposition rate, the temperatures found to optimize the growth were significantly different, i.e. 250 °C vs. 125 °C. Such discrepancy in the temperature is significant and cannot be explained by the inaccuracy of *in vacuo* temperature measurement. It suggests not only that each beam composition is unique and depends on the experimental setup, but also that the temperature of the substrate can effectively influence parameters, controlling such processes as: condensation of magnesium, condensation of oxygen, and nucleation of MgO. In effect, the rates of those processes can be controlled to some extent by the temperature of the sample, and optimal growth conditions can be potentially still reached.

The formation of the FeO_x layer has not been discussed here, as it is beyond the range of experimental methods used in this study. It was mentioned that an FeO_x layer can facilitate the epitaxial growth of MgO thin films on the Fe(0 0 1) surface [15]. Because of the direct exposure of the substrate to molecular oxygen, the interface must be partially oxidized. On the other hand, the high quality of MgO films indicates that the interfacial oxygen occupies only some fraction of a monolayer and does not lead to the formation of disordered iron oxide islands. From the thermodynamical point of view, the structure of the MgO/Fe interface is related to the interface contribution of an FeO_x layer to the surface energy, which decides the quality of layer-by-layer growth. The preferential quantity of FeO_x should be given by conditions that minimize the total energy of the system. Because the formation of FeO_x is governed by thermodynamics, it is expected to form to some extent regardless of the preparation method. Even a deposition of MgO by electron beam evaporation that is performed with special care to avoid the oxidation of the interface [32] leads to values of $x \approx 60\%$. In the reactive deposition method, this parameter must be significantly higher, but still does not exceed 100% as the Fe/MgO interface remains highly ordered.

4. Conclusions

The objective of this work was to use a reactive deposition method to improve the quality of MgO ultra-thin films grown on Fe(0 0 1) surfaces. We established a protocol that prevents an excessive interfacial reaction between oxygen and the Fe(0 0 1) surface, but at the same time provides sufficient amount of oxygen in order to grow a stoichiometric MgO film. We use the control over the gaseous species that reach the sample to either reduce the O_2 pressure at the beginning of the growth for a duration needed to grow the 1st MgO ML or to deposit a submonolayer coverage of Mg prior to the reactive growth of MgO. As revealed by LEED measurements, post-annealing of MgO films induces changes in the structure of misfit dislocations and flattening of the interface. Using NC-AFM we demonstrate that the reactive deposition method can produce terraces that have an average size of 10 nm, which is a significant improvement compared to other preparation methods.

References

[1] S. Yuasa, D.D. Djayaprawira, Journal of Physics D: Applied Physics 40 (2007) R337.
[2] G. Pacchioni, S. Valeri (Eds.), Oxide Ultrathin Films, Wiley, New York, 2012.
[3] S. Yuasa, T. Nagahama, A. Fukushima, Y. Suzuki, K. Ando, Nature Materials 3 (2004) 868.
[4] S.S.P. Parkin, C. Kaiser, A. Panchula, P.M. Rice, B. Hughes, M. Samant, S.-H. Yang, Nature Materials 3 (2004) 862.
[5] W. Butler, X.-G. Zhang, T. Schulthess, J. MacLaren, Physical Review B 63 (2001) 054416.
[6] J. Mathon, A. Umerski, Physical Review B 63 (2001) 220403.
[7] M. Klaua, D. Ullmann, J. Barthel, W. Wulfhekel, J. Kirschner, R. Urban, T. Monchesky, A. Enders, J. Cochran, B. Heinrich, Physical Review B 64 (2001) 134411.
[8] M. Mizuguchi, Y. Suzuki, T. Nagahama, S. Yuasa, Applied Physics Letters 88 (2006) 251901.
[9] J.L. Vassent, A. Marty, B. Gilles, C. Chatillon, Journal of Crystal Growth 219 (2000) 434.
[10] S. Schintke, S. Messerli, M. Pivetta, F. Patthey, L. Libioulle, M. Stengel, A. De Vita, W.-D. Schneider, Physical Review Letters 87 (2001) 276801.
[11] S. Benedetti, P. Torelli, S. Valeri, H. Benia, N. Nilius, G. Renaud, Physical Review B 78 (2008) 195411.
[12] C. Tegenkamp, M. Michailov, J. Wollschläger, H. Pfnür, Applied Surface Science 151 (1999) 40.
[13] X.-G. Zhang, W. Butler, A. Bandyopadhyay, Physical Review B 68 (2003) 092402.
[14] P. Bose, A. Ernst, I. Mertig, J. Henk, Physical Review B 78 (2008) 092403.
[15] A. Cattoni, D. Petti, S. Brivio, M. Cantoni, R. Bertacco, F. Ciccacci, Physical Review B 80 (2009) 104437.
[16] P. Blonski, A. Kiejna, J. Hafner, Physical Review B 77 (2008) 155424.
[17] F. Bonell, S. Andrieu, A. Bataille, C. Tiusan, G. Lengaigne, Physical Review B 79 (2009) 224405.
[18] S.S. Parihar, H.L. Meyerheim, K. Mohseni, S. Ostanin, A. Ernst, N. Jedrecy, R. Felici, J. Kirschner, Physical Review B 81 (2010) 075428.
[19] H. Oh, S.B. Lee, J. Seo, H.G. Min, J.-S. Kim, Applied Physics Letters 82 (2003) 361.
[20] M. Müller, F. Matthes, C.M. Schneider, Europhysics Letters 80 (2007) 17007.
[21] M. Müller, F. Matthes, C.M. Schneider, Journal of Applied Physics 101 (2007) 09G519.
[22] O. Dugerjav, H. Kim, J.M. Seo, AIP Advances 1 (2011) 032156.
[23] R.N. Gardner, Journal of Crystal Growth 43 (1978) 425.
[24] I. Colera, E. Soria, J. de Segovia, E. Román, R. González, Vacuum 48 (1997) 647.
[25] J.A. Venables, Introduction to Surface and Thin Film Processes, Cambridge University Press, Cambridge, 2000.
[26] M. Dynna, J.L. Vassent, A. Marty, B. Gilles, Journal of Applied Physics 80 (1996) 2650.
[27] J. Wollschlager, D. Erdos, K.-M. Schroder, Surface Science 402–404 (1998) 272.
[28] J. Wollschlager, D. Erdos, H. Goldbach, R. Hopken, K. Schroder, Thin Solid Films 400 (2001) 1.
[29] R. Urban, Electron tunneling and spin dynamics and transport in crystalline magnetic multilayers, Simon Fraser University, Burnaby, B.C., PhD thesis, 2003.
[30] W. Han, Y. Zhou, Y. Wang, Y. Li, J.J.I. Wong, K. Pi, A.G. Swartz, K.M. McCreary, F. Xiu, K.L. Wang, J. Zou, R.K. Kawakami, Journal of Crystal Growth 312 (2009) 44.
[31] K.-R. Jeon, C.-Y. Park, S.-C. Shin, Crystal Growth and Design 10 (2010) 1346.
[32] C. Tusche, H. Meyerheim, N. Jedrecy, G. Renaud, J. Kirschner, Physical Review B 74 (2006) 195422.